1	MAGE Model Simulation of the Pre-reversal Enhancement and Comparison with ICON and
2	Jicamarca ISR Observations
3	
4	Qian Wu ¹ , Wenbin Wang ¹ , Dong Lin ¹ , Liying Qian ¹ , Chaosong Huang ² , and Yongliang Zhang ³
5	
6	¹ High Altitude Observatory, National Center for Atmospheric Research, Boulder, CO, USA
7	² Space Vehicles Directorate, Air Force Research Laboratory, Kirtland AFB, New Mexico, USA
8	³ Applied Physics Laboratory, Johns Hopkins University, Laurel, MD, USA
9	
10	Abstract
11	Using the latest coupled geospace model MAGE (Multiscale Atmosphere-Geospace Environment)
12	and observations from Jicamarca ISR and ICON IVM instrument, we examine the pre-reversal
13	enhancement during geomagnetic quiet time period. The MAGE shows comparable PRE to both
14	the Jicamarca ISR and ICON observations. There appears to be a discrepancy between the
15	Jicamarca ISR and ICON IVM with the later showed PRE about two times larger (~ 40 m/s). This
16	is the first time that MAGE is used to simulate the PRE. The results show that the MAGE can
17	simulate the PRE well and are mostly consistent with observations.
18	
19	Introduction
20	Pre-reversal enhancement (PRE) is a prominent feature of the equatorial ionosphere near dusk and
21	has been studied extensively with simulations and observations [e.g., Fejer et al., 1991; 2007].
22	PRE plays a critical role in the occurrence of plasma bubbles as it is directly related to the
23	Rayleigh-Taylor instability growth rate [e.g., Sultan, 1996; Wu, 2015; 2017]. Hence, the capability

to reproduce PRE in numerical simulation is a critical component for model development. The Multiscale Atmosphere-Geospace Environment (MAGE) model is a whole geospace model that has been developed at the NASA DRIVE Science Center for Geospace Storms [Pham et al., 2022; Lin et al., 2021; 2022]. MAGE has been widely used in studies on magnetosphere-ionospherethermosphere coupling during storm time [e.g., Lin et al., 2022a; 2022b; Wu et al., 2022; Shi et al., 2022]. The MAGE model is featured by its capability to resolve mesoscale structures and processes in the coupled magnetosphere-ionosphere and represent dynamic magnetospheric forcing in the high latitude ionosphere. Because PRE is an important feature of the ionosphere strongly related to the space weather, it will be very useful to compare the MAGE simulation of the PRE with the observations from recent satellite mission and ground-based instruments. For this purpose, we selected a time interval when the Jicamarca incoherent scatter radar (11.7S, 76.7W) [Farley, 1991] and NASA ICON IVM [Immel et al 2018; Heelis et al. 2017] observations were available. The paper is organized as follows. First, we provide a brief description of the MAGE model, ICON IVM, and Jicamarca ISR instruments. Then, we will show the comparison of the MAGE simulations with the Jicamarca ISR and with ICON IVM observations for the selected time periods September 21 and 22, 2020. We will discuss the results and summarize our findings.

40

41

42

43

44

45

46

24

25

26

27

28

29

30

31

32

33

34

35

36

37

38

39

MAGE Model

MAGE model is driven by the Grid Agnostic MHD with Extended Research Application (GAMERA) magnetosphere model [Zhang et al., 2019] and coupled with the NCAR TIEGCM (Thermosphere Ionosphere Electrodynamics General Circulation Model, Richmond et al., 1992) incorporating the RCM [Rice Convection Model, Toffoletto et al., 2003] to simulate the ring current effect. The potential map from GAMERA is connected to the TIEGCM using REMIX

- 47 (RE-developed Magnetosphere-Ionosphere Coupler/Solver, Merkin and Lyon, 2010). The 48 simulation used in this study is driven by CDAWeb OMNI database with one-minute resolution. 49 The TIEGCM is set with 1.25 degree latitudinal and longitudinal resolution with 0.25 scale height.
- 50 The 57 vertical grid covers from \sim 96 km to \sim 600 km. The simulation time step of TIEGCM
- within MAGE is 5 seconds and results are saved every 5 minutes.

53

ICON IVM

ICON was a NASA equatorial ionospheric connection mission [Immel et al, 2018]. It carried an ion velocity meter (IVM) instrument [Heelis et al., 2017]. The IVM instrument provides ExB ion drift in the meridional direction. At the magnetic equator, the ExB meridional drift will be upward zenith pointing. Not far off the magnetic equator, the ExB meridional drift is a good approximate for the vertical ion drift. IVM samples the drift with 1 sec resolution.

59

60

Jicamarca ISR

- 61 Jicamarca Incoherent scatter radar (ISR) operates at 50MHz, with very high altitude reach (\sim 6000
- 62 km [Farley, 1991]. The Jicamarca ISR is located very close the magnetic equator at 11.95N,
- 63 76.87W and is often used to measure vertical ion drift and pre-reversal enhancement (PRE).

64

65

66

67

68

69

Simulations and Observations

The time periods of September 21 and 22, 2020 were selected for analysis of the PRE with observations from Jicamarca ISR and ICON IVM instruments and MAGE simulation. Figure 1 shows the IMF data for September 21, 2020. Throughout the day the IMF Bz stayed mostly positive. There is no indication of geomagnetic activities as shown by the SYM/H values. Solar

wind speed was low (< 300 m/s). Figure 2 shows the comparison between the Jicamarca ISR vertical ion drift during September 21, 2020. The local time is 5 hours behind the UT. UT (Jicamarca 19 LT), the vertical ion drift clearly shows a pre-reversal enhancement. The MAGE simulated Jicamarca vertical ion drift also show a clear PRE about twice the size. Overall, the MAGE simulations have similar feature from the Jicamarca ISR. Only on the dayside the upward ion drift from the MAGE is about half of what observed by the ISR. The comparison looks pretty good in general. Because ground base observation is at a fixed location, it will take the whole day to see the local time variation of the ion drift. A fast moving satellite like ICON can sample all local times in one orbit, although at different longitudes. An orbit lasts about 90 minutes for a low earth orbit satellite like ICON. Because we would like to compare the ion drift around 18 LT to see PRE, we selected the interval within 23 to 24 UT, which coincides with overpass of American sector close to Jicamarca, as highlighted in Figure 2 for comparison with ICON observation. Figure 3 shows the ICON IVM EXB meridional drift data between 23:15 to 23:55 UT. In the plot we also indicated the local time and longitude as the ICON satellite moved across the space. The longitudes, local time and UT are given below the plot. The vertical ion drifts from ICON IVM clearly show PRE near 18 LT. Jicamarca is located 284E longitude coincide with PRE. The MAGE simulation also displayed strong PRE at the same local time and location. While satellite can sample all location in ~ 90 minutes, MAGE can produce simulations of all local times at any UT. We can view the instantaneous pattern of the vertical ion drift globally or regionally. To examine the regional view of the vertical ion drift from the model when ICON flew close to Jicamarca and also to give a view of ICON satellite track in longitudes and latitudes, Figure 4 shows the MAGE simulation of ExB vertical ion drifts at the magnetic equator, along the ICON satellite track (black line above and below the satellite track), and ICON IVM observation

70

71

72

73

74

75

76

77

78

79

80

81

82

83

84

85

86

87

88

89

90

91

of (cyan and magenta vectors). The observed and simulated EXB meridional ion drift covers about 40 minutes. The IVM data corresponding the moment of the regional simulation at 2349 UT are shown in magenta color.

We have shown that the PRE as a feature vs local time from one day period at fixed ground based location, from a moving low inclination satellite, and from one instance in the simulation and in all these perspectives the MAGE and observations are mostly consistent. We further examine the data from the next day September 22, 2020, in the same format as in the case of September 21, 2020.

The IMF parameters for September 22, 2020 are displayed in Figure 5. The IMF Bz was mostly negative before 17 UT and near zero afterward. The IMF By was mostly negative before 10 UT and mostly positive thereafter. The solar wind speed and density were not in any storm conditions. The SYM/H showed no indication of the substorm activity. These parameters show this is mostly quiet day.

Figure 6 shows the MAGE simulation comparison with the Jicamarca ISR vertical ion drift comparison of September 22, 2020 in the same format as Figure 2. This case is very similar to the case of September 21 and the PRE is also clearly shown in both the MAGE simulation and Jicamarca ISR data. In addition, both simulations and observations showed negative vertical ion drift before noon. Different from the September 21 case, the timing of the variations in the MAGE simulation is slightly ahead of the observations. The PRE from both MAGE and ISR are

about ~20 m/s. The time interval highlighted near the PRE is for more comparison between the model and ICON IVM observations from 2322 to 2359UT shown in Figure 7.

Figure 7 is a comparison between the MAGE simulation and ICON IVM observation on September 22 in the same format as Figure 3. The PRE in the simulation and ICON IVM observation occurred at about the same time after 2352 UT. The MAGE simulated PRE is only half of that from the ICON IVM. The ICON IVM observed PRE vertical ion drifts (~ 40 m/s) were much larger than that from the MAGE model and the Jicamarca ISR observed values (~ 20 m/s) in Figure 6. The highlighted interval is for comparison of the model and ICON observations at the instance of the ICON passing the PRE to be shown in Figure 8.

Figure 8 shows the simulated vertical ion drifts at the magnetic equator at 2355 UT. The simulation results at the instance also show PRE clearly. But the simulated PRE is smaller than that observed by the ICON IVM. Also plotted in the figure are the ICON IVM sampled ExB meridional ion drift and the sampled MAGE simulation also the ICON orbit. The ICON orbit covers the same time period shown in Figure 7. In the plot we can see that the ICON was sampling at about 20 deg magnetic latitude. The NmF2 of the of the MAGE simulation is also plotted. The EIAs are enhanced in the afternoon as expected. The simulated PRE is smaller than that in September 21.

Discussions

In these two days, the PRE are clearly seen in the MAGE simulations, as well as in the ICON IVM and Jicamarca ISR observations. The agreement between the MAGE simulation and observation

are reasonably good. We examine the observation on one day (with ISR), one orbit (ICON IVM, ~90 minutes), and one instance (ICON IVM) time scales. The PRE is a persistent feature in all three. The time period we examine is in fall equinox, which is a time period for high bubble occurrence associated with strong PRE. The geomagnetic activity is low during the two days in general, hence the PRE is not associated the substorms and more in line with the seasonal variations of the equatorial dynamo that induces PRE.

144

145

146

138

139

140

141

142

143

ICON IVM and Jicamarca ISR Comparison

- It appears that the ICON IVM observed PRE are larger than the Jicamarca ISR observed values.
- On September 21, Jicamarca ISR observed ~ 10 m/s, whereas ICON IVM showed ~ 20 m/s. On
- 148 September 22, the ISR showed about ~ 20 m/s and ICON IVM ~ 40 m/s. IVM instrument on the
- 149 C/NOFS satellite had been compared with the Jicamarca ISR [Stoneback et al., 2012] and in the
- 150 comparison the agreement was very good. It is unclear why there seems be a significant
- discrepancy with the ICON IVM.

152

153

MAGE and Jicamarca ISR Comparison

- 154 The MAGE simulation was able to reproduce the PRE. The PRE from MAGE is larger than that
- from the ISR on September 21 (~ 20 m/s vs ~ 10 m/s), whereas on September 22, they are about
- the same ($\sim 20 \text{ m/s}$). As a first principle model, the agreement is very good given the discrepancy
- in the two sets of observations.

158

159

MAGE and ICON IVM Comparison

The MAGE comparison with ICON IVM is opposite in agreement vs the comparison with the ISR. The comparison on September 21 showed the MAGE agree with ICON IVM observed PRE (\sim 20 m/s), whereas on September 22, the MAGE underestimated the PRE (\sim 20 m/s vs \sim 40 m/s). The degree of consistency between the MAGE simulation and ICON IVM is about the same. Sometime, the MAGE agrees better with the ISR and other times with ICON IVM.

Overall the MAGE model demonstrates the capability of simulation of PRE. As to the agreement with observations, the MAGE simulation sometimes agree with the ISR better than ICON IVM and vice versa. Given there appears to be some kind of discrepancy between two sets of observations, the MAGE simulation did not show any preference to one over the other. It is unclear if the PRE discrepancy (IVM vs ISR) is a persistent feature or not as past comparison between the C/NOFS IVM and Jicamarca ISR did not show such a difference.

Summary

We examined the PRE during mostly quiet geomagnetic conditions based on the MAGE simulations and observations from ground based Jicamarca ISR and satellite based ICON IVM instrument. We found that 1. The MAGE is able to simulate the PRE very well. 2. The PRE was a persistent feature on different time scales (day, hour, and minute) during this fall equinox time period. 3. Jicamarca ISR observed PRE is about half of size of that by the ICON IVM. 4. MAGE simulated sometime agree with the Jicamarca ISR observation and at other time with ICON IVM.

Acknowledgement

182 This research is supported from NASA grants 80NSSC20K0199, 80NAAC21K0014, 183 NNX17AG69G and NSF grants AGS-2120511 and AGS-2054356. W. Wang is supported by 184 NASA grants 80NSSC20K0601, 80NSSC17K0013,80NSSC20K0356, 80NSSC19K0080, 185 80NSSC17K0679, and 80NSSC20K0199. D. Lin is supported by 80NSSC17K0013, 186 80NSSC21K0008, 80NSSC20K0601, 80NSSC21K1677. L. Qian is supported by NASA grants 187 80NSSC20K0189. C. Huang is supported by NASA grants 80HQTR20T0016, 80HQTR20T0015, 188 and NNH22OB17A. Y. Zhang is supported by NASA grant 80NSSC20K0354 and 189 80NSSC21K1673. NCAR is supported by National Science Foundation. Jicamarca ISR data can 190 be obtained from the CEDAR madrigal database (http://cedar.openmadrigal.org/). ICON IVM 191 data can be obtained from the ICON data server (https://icon.ssl.berkeley.edu/Data). The 192 simulation data can be found at (https://doi.org/10.5065/e4n6-gp28) 193 194 195 References 196 197 Farly, D. T. (1991), Early incoherent scatter observations at Jicamarca, J. Atmos. Terr. Phys., 53, 198 665-675, https://doi.org/10.1016/0021-9169(91)90120-V 199 Fejer, B. G., de Paula, E. R., González, S. A., and Woodman, R. F. (1991), Average vertical and 200 zonal F region plasma drifts over Jicamarca, J. Geophys. Res., 96(A8), 13901-13906, 201 202 doi:10.1029/91JA01171. 203

- Fejer, B. G., Jensen, J. W., Kikuchi, T., Abdu, M. A., and Chau, J. L. (2007), Equatorial Ionospheric
- Electric Fields During the November 2004 Magnetic Storm, J. Geophys. Res., 112, A10304,
- 206 doi:10.1029/2007JA012376.

- Heelis, R.A., Stoneback, R.A., Perdue, M.D. et al. Ion Velocity Measurements for the Ionospheric
- 209 Connections Explorer, Space Sci Rev 212, 615–629 (2017). https://doi.org/10.1007/s11214-017-
- 210 0383-3.

- Immel et al., (2018), The Ionospheric connection explorer mission: Mission Goals and design,
- 213 Space Sci. Rev., doi:/10.1007/s11214-017-0449-2.
- Lin, D., Sorathia, K., Wang, W., Merkin, V., Bao, S., Pham, K., et al. (2021). The role of diffuse
- electron precipitation in the formation of subauroral polarization streams. *Journal of Geophysical*
- 216 Research: Space Physics, 126, e2021JA029792. https://doi.org/10.1029/2021JA029792.
- Lin, D., Wang, W., Merkin, V. G., Huang, C., Oppenheim, M., Sorathia, K., et al. (2022). Origin
- of dawnside subauroral polarization streams during major geomagnetic storms. AGU Advances,
- 3, e2022AV000708. https://doi.org/10.1029/2022AV000708
- Merkin, V., & Lyon, J. (2010). Effects of the low-latitude ionospheric boundary condition on the
- 221 global magnetosphere. Journal of Geophysical Research: Space Physics, 115(A10). doi:
- 222 10.1029/2010JA015461.
- Pham, K. H., Zhang, B., Sorathia, K., Dang, T., Wang, W., Merkin, V., et al. (2022). Thermospheric
- density perturbations produced by traveling atmospheric disturbances during August 2005 storm.

- 225 Journal of Geophysical Research: Space Physics, 127, e2021JA030071.
- 226 https://doi.org/10.1029/2021JA030071
- Richmond, A., Ridley, E., & Roble, R. (1992). A thermosphere/ionosphere general circulation
- 228 model with coupled electrodynamics. Geophysical Research Letters, 19(6), 601-604. doi:
- 229 10.1029/92GL00401.
- Sultan, P. J. (1996), Linear theory and modeling of the Rayleigh-Taylor instability leading to the
- occurrence of equatorial spread F, J. Geophys. Res., 101(96), doi:10.1029/96JA00682.
- Toffoletto, F., Sazykin, S., Spiro, R., & Wolf, R. (2003). Inner magnetospheric modeling with the
- 233 rice convection model. Space Science Reviews, 107(1-2), 175–196. doi:
- 234 10.1023/A:1025532008047.

- Wang, W., J. Lei, A. G. Burns, M. Wiltberger, A. D. Richmond, S. C. Solomon, T. L. Killeen, E.
- 236 R. Talaat, and D. N. Anderson (2008), Ionospheric electric field variations during a geomagnetic
- storm simulated by a coupled magnetosphere ionosphere thermosphere (CMIT) model, *Geophys*.
- 238 Res. Lett., 35, L18105, doi:10.1029/2008GL035155.
- 240 Wu, Q., Wang, W., Lin, D., Huang, C., & Zhang, Y. (2022). Penetrating electric field simulated
- by the MAGE and comparison with ICON observation. *Journal of Geophysical Research: Space*
- 242 *Physics*, 127, e2022JA030467. https://doi.org/10.1029/2022JA030467

244 Wu, Q. (2015), Longitudinal and seasonal variation of the equatorial flux tube integrated Rayleigh-Taylor instability growth rate, J. Geophys. Res. Space Physics, 120, 7952–7957, 245 doi:10.1002/2015JA021553. 246 247 Wu, Q. (2017), Solar effect on the Rayleigh-Taylor instability growth rate as simulated by the 248 NCAR TIEGCM, J. Atmos. Solar-Terrestrial Phys., 156, 97–102, 249 doi:10.1016/j.jastp.2017.03.007. 250 Zhang, B., Sorathia, K. A., Lyon, J. G., Merkin, V. G., Garretson, J. S., & Wiltberger, M. (2019). 251 GAMERA: A three-dimensional finite-volume MHD solver for non-orthogonal curvilinear geometries. The Astrophysical Journal Supplement Series, 244(1), 20. doi: 10.3847/1538-252 253 4365/ab3a4c. 254 255 256 Figure captions

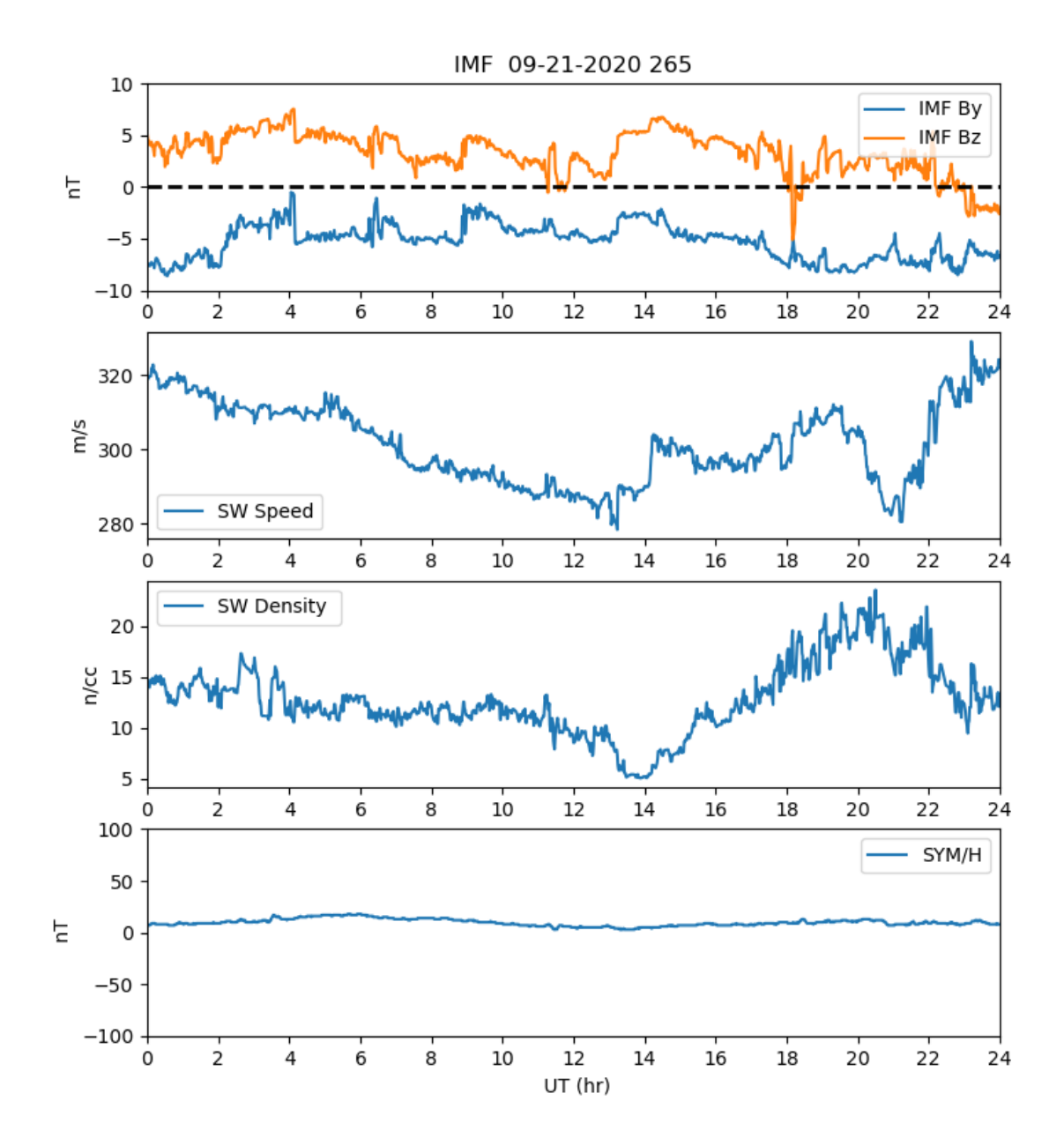


Figure 1. IMF Bz and By (first panel), solar wind speed (second panel), density (third panel), and SYM/H for September 21, 2020. IMF Bz stayed mostly positive resulting in mostly quiet condition as indicated by smooth SYM/H.

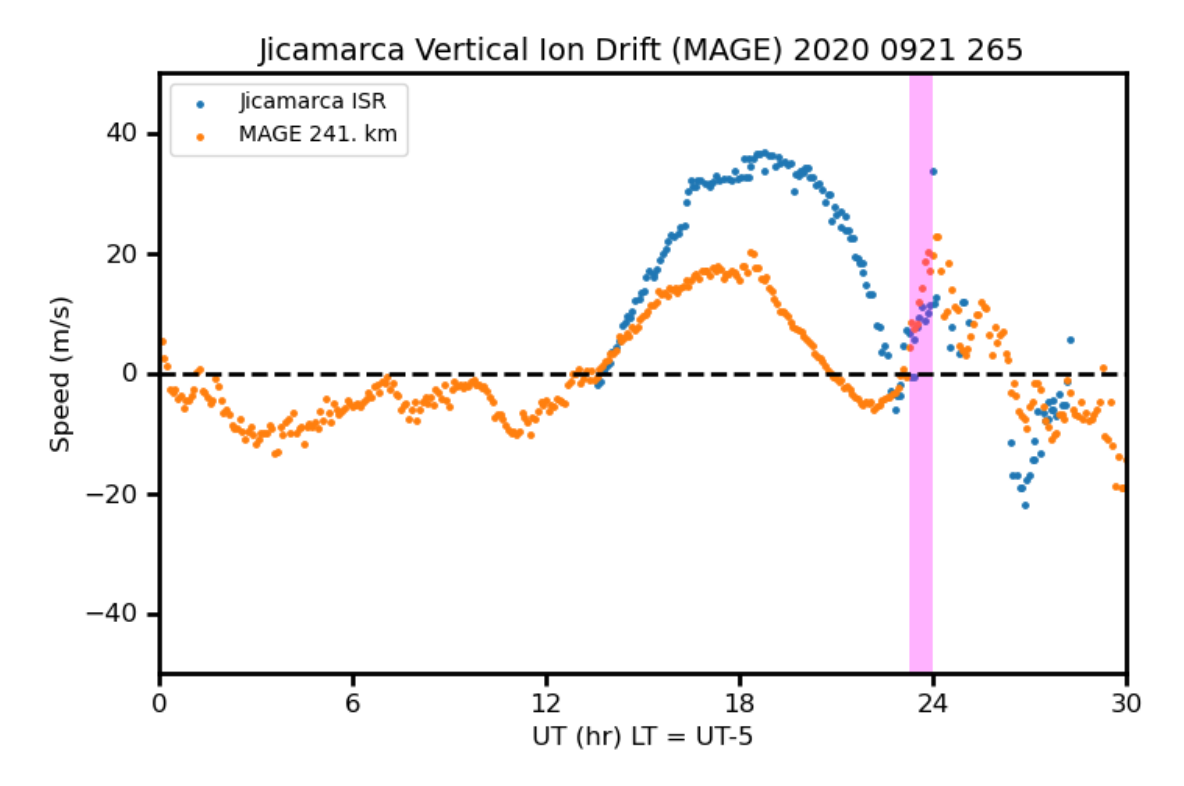


Figure 2. Comparison of MAGE simulation and Jicamarca Incoherent scatter radar (ISR) vertical ion drifts during September 21-22, 2020. The highlighted period coinciding with the PRE near 24 UT of September 21, 2020. The MAGE data are sampled at the location of Jicamarca for comparison with the ISR observation. This highlighted period will be investigated with the MAGE simulation and ICON IVM observations.

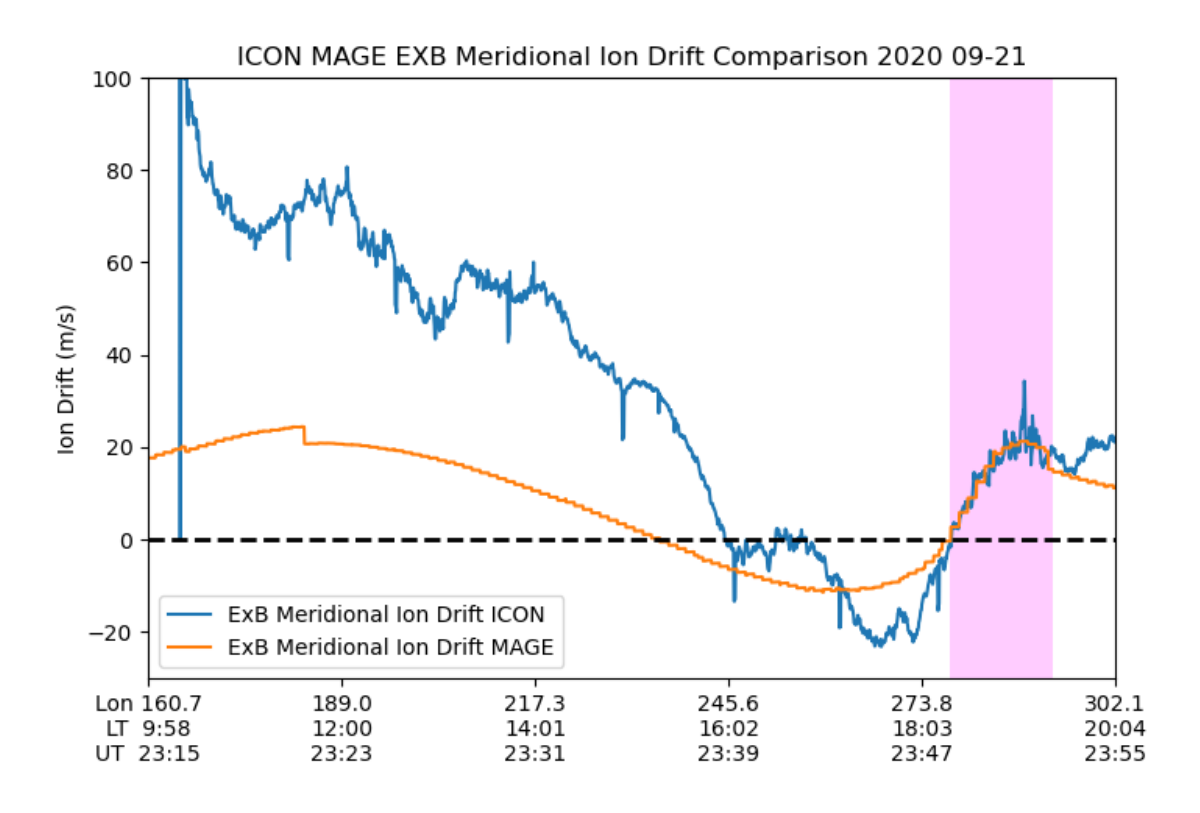


Figure 3. Comparison of meridional ion drift measured by ICON and simulated by MAGE. The MAGE results are sampled along ICON satellite trajectory. Along the UT, the local time and longitudes along the ICON orbit are also provided. The MAGE simulation was sampled along the ICON orbit track for comparison with ICON IVM observations. The PRE is very clear between 23:47 to 23:55 UT of the orbit track.

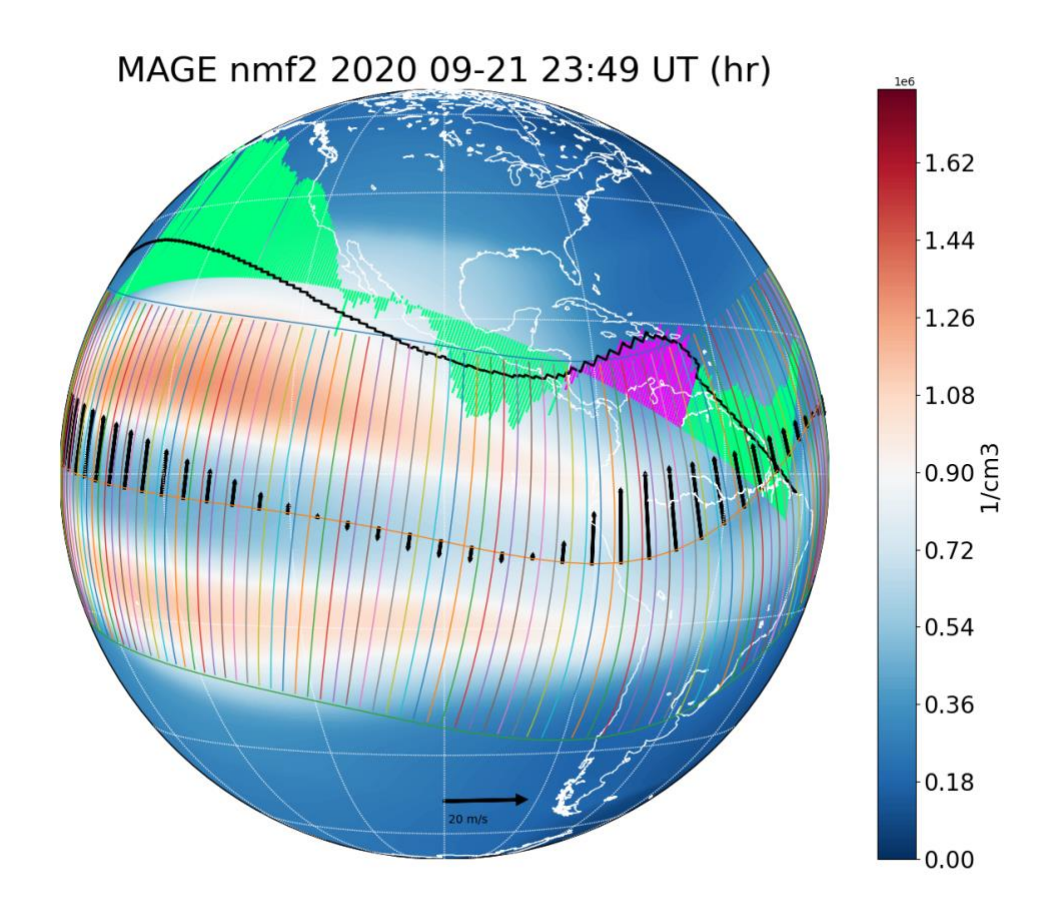


Figure 4. MAGE simulations of the equatorial vertical ion drifts (black vectors along the magnetic equator) at 23:49 UT sampled along the ICON satellite track (black line above the satellite track) and IVM observation (lime or magenta vector) from 23:15 to 23:55 UT. The magenta vectors are for the 2349 UT. The PRE is visible in both the equatorial vertical ion drift and along the satellite tracks. The background shows the nmf2 from the MAGE simulation.

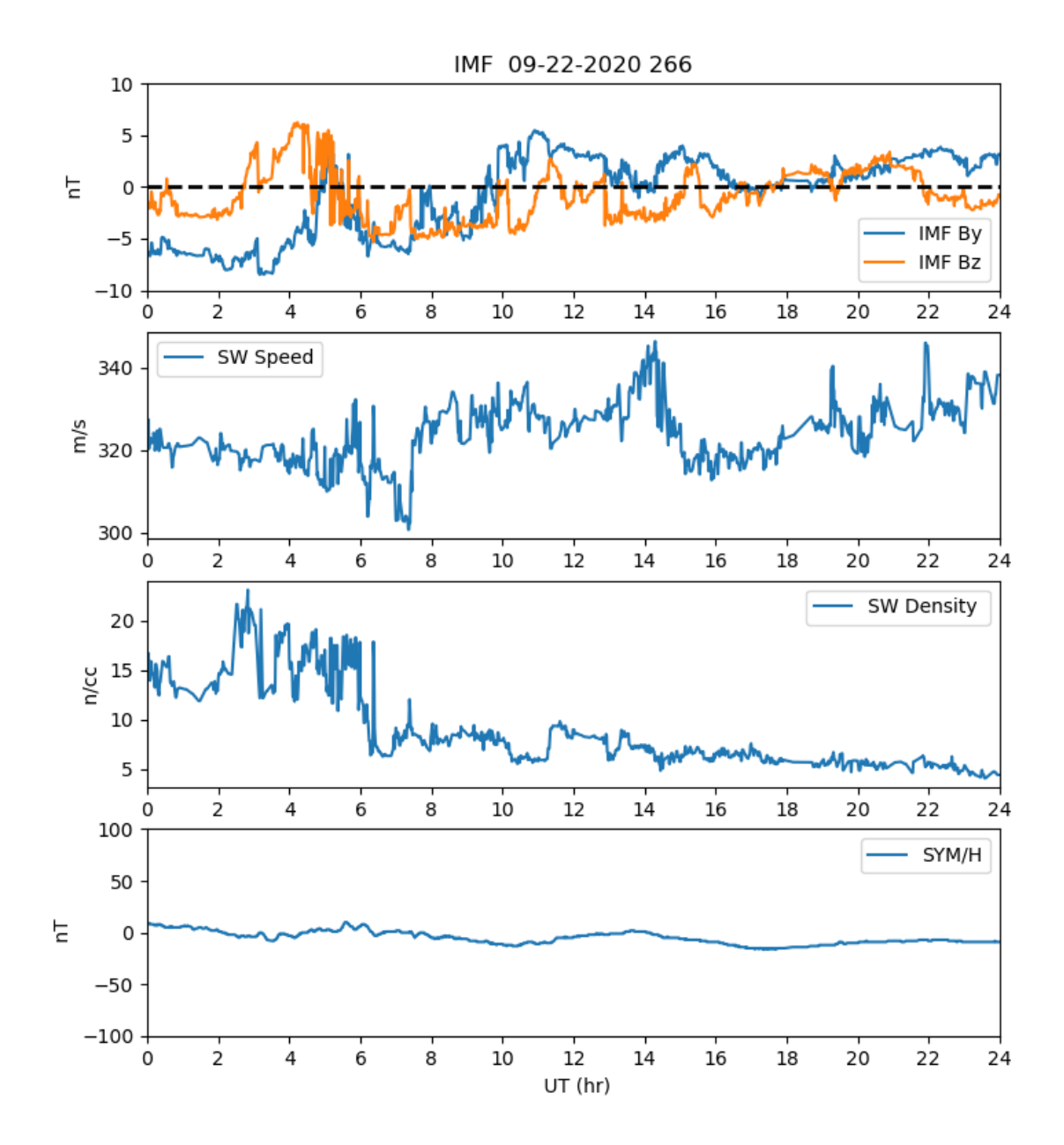


Figure 5. IMF and Solar wind parameters for September 22, 2020. Same as Figure 1 but for September 22, 2020. Although the IMF Bz was slightly negative, there was no geomagnetic activities as indicated by mostly smooth SYM/H. Solar wind speed is low at \sim 300 m/s and density is not high < 10 n/cc.

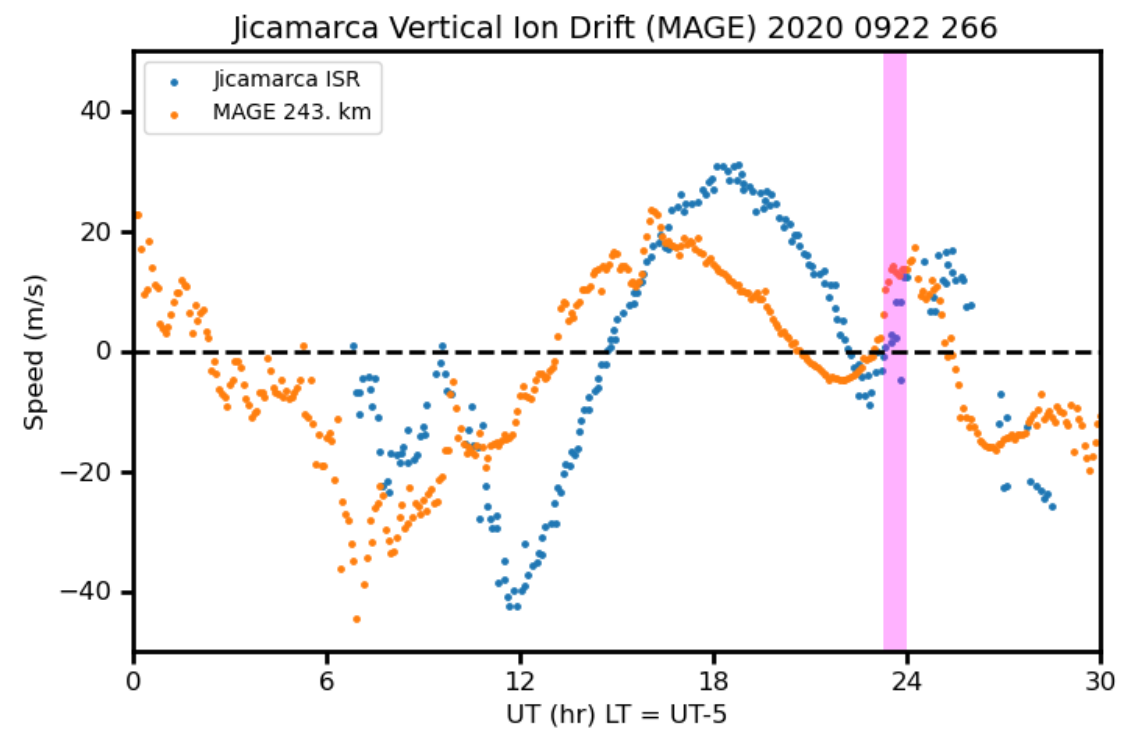


Figure 6. Same as Figure 2 but for September 22, 2020.

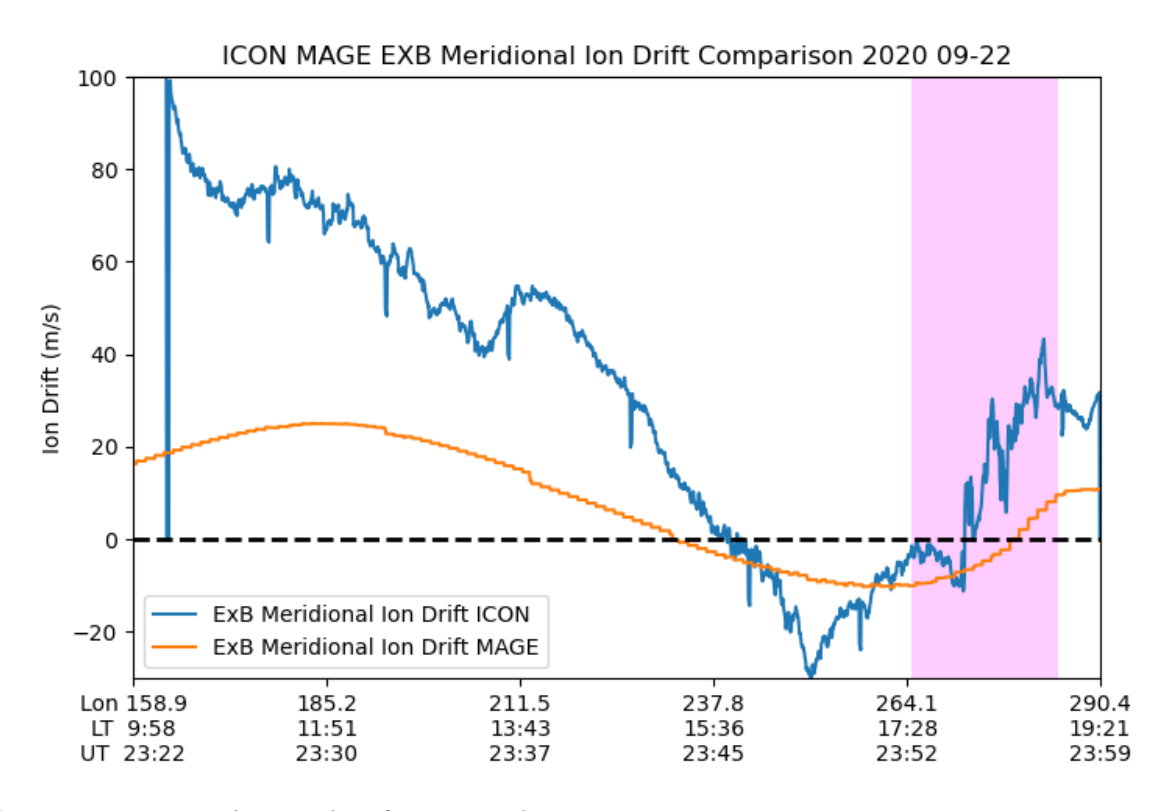


Figure 7. Same as Figure 3 but for September 22, 2020.

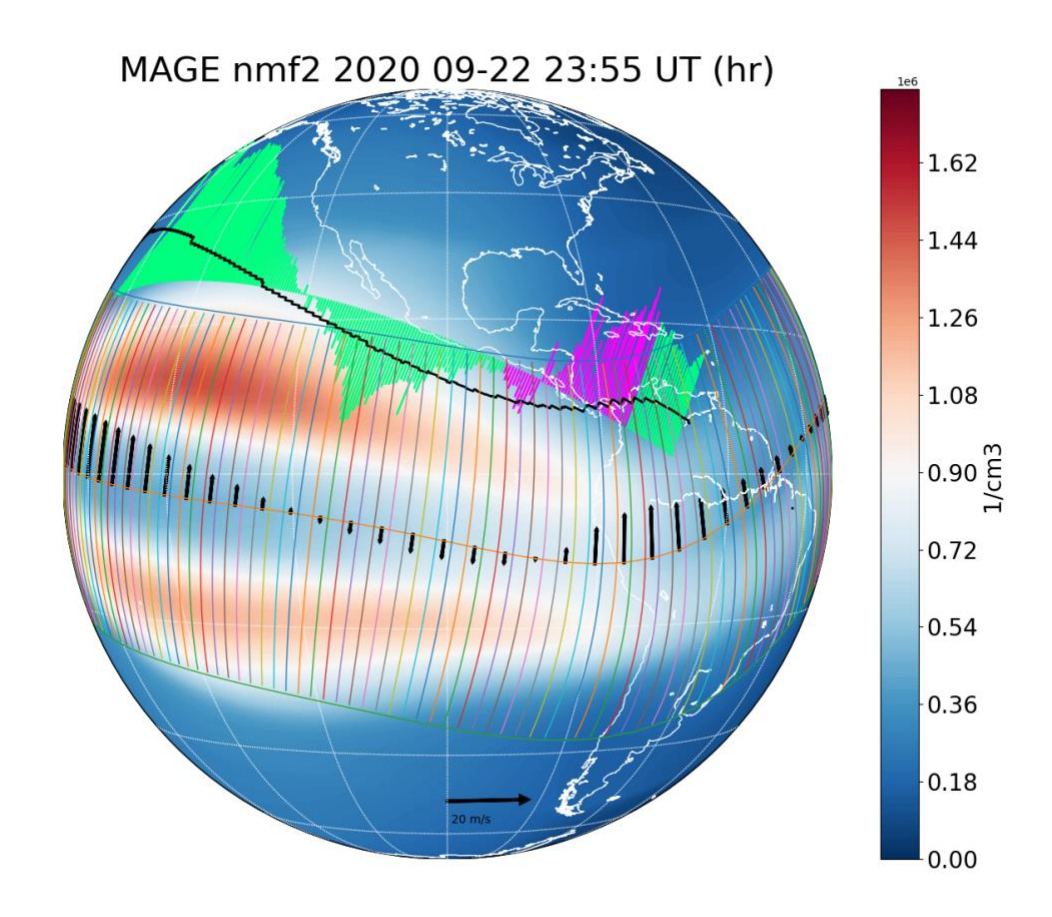


Figure 8. Same as Figure 4 but for September 22, 2020.